Monte Carlo Simulation of Schottky Barrier Mixers and Varactors

J. East[1]
Center for Space Terahertz Technology
The University of Michigan
Ann Arbor, Michigan 48109

Abstract

Current saturation effects can be an important limitation on the performance of Schottky barrier mixers and multipliers. This effect was first discussed at this conference in 1991 with additional results in 1993 and 1994. These earlier results are all based on a static or equilibrium description of the device. This paper will describe a large signal Monte Carlo simulation of Schottky barrier mixers and varactors. The simulation is a time dependent particle field Monte Carlo simulation with ohmic and Schottky barrier boundary conditions included. The simulation will be used to point out some important time constants in GaAs and to describe the effects of current saturation due to valley transfer in GaAs varactors and inductive delay and current saturation effects in very high frequency mixers.

I. Introduction

Schottky barrier diodes are critical components in millimeter and submillimeter wave receiver systems. They are used in multipliers with input and output frequencies of hundreds of GHz and in receivers to THz frequencies. Mixer and multiplier modeling is needed to better understand the performance of these devices and to design circuits. Several modeling tools are available[1-3]. The modeling is usually a combination of a linear frequency domain description of the circuit and a nonlinear time domain description of the device. The approaches use harmonic balance or multiple reflection techniques. They start with an approximation for the voltage waveform across the devices and frequency domain information about the circuit and time evolve to a final approximation for the voltage and current waveforms at the device terminals. These techniques require a description of the active device. A lumped element model with voltage dependent elements is typically used. Measured low frequency data or calculated information for the capacitance and current vs. voltage can be used. The performance also depends on the series resistance which

[1]This work was supported by the Center for Space Terahertz Technology under contact No. NAGW-1334

be either calculated or measured. The series resistance is sometimes also frequency dependent. This approach has been used to study mixer and multiplier performance over a wide range of frequencies. The match between theory and experiment is encouraging at lower frequencies. However, as the frequency or power levels go up the predicted powers and efficiencies are typically lower than experimental results. There are several possible explanations. High frequency circuits are small and difficult to fabricate. Skin effect and backshort losses both go up with frequency. These losses can be taken into account in the simulation, but the required loss values tend to be relatively large when compared with other information about waveguide and mount loss. The impedance presented to the device by the circuit is sometimes inferred from scale model measurements at much lower frequencies. As the operating frequency increases mechanical tolerance limitations and loss make it much more difficult to predict operating conditions from scale models. Another problem is the nonlinear circuit used to describe the diode. Another problem is the lump element model for the nonlinear device.

A simple lumped element equivalent circuit can have problems representing the device operation at high frequencies. A paper by Kollberg et al[4] described saturation effects in varactors using a lumped element representation for the varactor with elements that depended on the current level. This approach was also used by to model multipliers by Louhi and Raisanen[5] and experimentally to design varactors by Crowe et. al.[6]. A paper by East et. al.[7] described a more detailed physical model for the saturation effects. That paper used a static velocity vs. electric field electron transport model to investigate saturation. A Monte Carlo based device simulation to further investigate device operation will be described in this paper.

The paper is organized as follows. The next section will discuss the implementation of a Monte Carlo simulation of Schottky barrier mixers and varactors. Several characteristic times that are important for varactor and mixer operation will be discussed. Section III will describe the Monte Carlo simulation of varactors. Section IV will describe THz mixer simulation. The paper will be summarized in Section V.

Monte Carlo Device Simulation

The effects under investigation occur at the high frequencies and electric field levels where the lumped element circuit approximation for the semiconductor device no longer applies. This section will describe a Monte Carlo based device simulation that can be used to investigate a range of frequencies and RF drive levels in order to get a better physical understanding of the device operation. A Monte Carlo simulation follows the motion of a collection of individual electrons as they move in a

semiconductor as a function of position and time. The details of the electron transport are represented by random variables with distributions that match the underlying physics of the transport. A Monte Carlo simulation typically follows the motion of many electrons to obtain average values for variables of interest. Descriptions of the Monte Carlo technique are given by Fawcett[8] and by Hochney and Eastwood[9]. The advantage of the Monte Carlo technique is a better physical description of the device operation and the disadvantage is the large amount of computer time needed. A Monte Carlo Schottky barrier device simulation has been written and will be discussed next.

A particle field Monte Carlo simulation has been modified to investigate the varactors and mixers of interest in this paper. The code uses a two valley parabolic band approximation for the GaAs. The details of the physics are taken from Fawcett[8]. The simulation steps the electrons and the solution of Poissons' equation as a function of time to obtain terminal characteristic. The code has been modified to investigate Schottky barrier devices. The boundary conditions have been modified to approximate a Schottky barrier diode. Electron flow out of the Schottky barrier end of the device during a time step. These electrons, along with the ones that flow out of the ohmic contact are available to be reintroduced at the ohmic contact at the end of each time steps. Electron in equilibrium with the contact field are added or eliminated from the contact to form a charge neutral ohmic contact at the start of each time step. Thus the number of electrons in the structure is a function of time. This simulation is an approximation to more complete codes that better describe the transport physics and the details of emission over the thermionic barrier[10]. However, it allows full device simulations with reasonable amounts of computer time. A typical simulation involving 10,000 initial electrons for 10 picoseconds corresponding to 100 GHz operation takes about several minutes per RF period. Fourier transforms of information for successive RF periods are compared until steady state results are obtained.to decay .

There are several characteristic times for semiconductor materials that effect the operation of mixers and multipliers. Before the details of the Monte Carlo results are described, it is informative to discuss these time scales, and the resulting nonequilibrium effects that modify device performance. The nonequilibrium effects include velocity saturation, valley transfer delays and inductive delays in the electron motion for rapidly changing electric fields. Varactors are usually operated as reverse biased diodes with relatively large RF voltage levels across the device. Frequency multipliers have input frequencies in the several hundred GHz range with corresponding time scales of one to ten picoseconds. Velocity saturation and valley transfer delays are important effects in these devices. Mixers are needed into the THz range, with corresponding time scales between several picoseconds and a fraction of a picosecond. They are usually forward biased with much lower RF power levels than

varactors. Inductive effects are important for these devices, with velocity saturation and valley transfer effecting the very high frequency operation. The Monte Carlo program can be used to investigate these characteristic times in a bulk GaAs structure.

One important time scale is the energy relaxation time or valley transfer time. Valley transfer occurs when electrons are heated by moderate electric fields. The time response of electrons in GaAs to an electric field switching slowly between one and twenty 20 KV/cm square wave is shown in Fig. 1. Fig. 1a shows the fraction of the electrons in the high mobility Γ valley as a function of time for the field shown in Fig. 1b. There are two important times, the time required to heat the electrons up enough to transfer to the upper valley and the corresponding cooling time required to relax again. The heating time is relatively short, a fraction of a picosecond, but the cooling time is about 2.75 picoseconds for GaAs. This corresponds to a frequency of about 60 GHz in GaAs. If the time scale is reduced, the electrons do not return to the Γ valley. This is shown in Fig. 1c and 1d for a total simulation time of twenty picoseconds. These valley transfer delays are well understood in the operation of Gunn devices and are a major limitation in their high frequency operation[11,12]. In a Gunn device a rapid transfer of electrons from valley to valley under a changing electric field is needed. The frequency response of GaAs based Gunn devices is limited to frequencies below 80 - 100 GHz because of the slow return of electrons from the upper valley. These valley response times also limit the performance of GaAs based varactors. A varactor consists of a depletion region and a bulk quasi-neutral region. The terminals of the device are pumped with a changing RF voltage which changes the width of the depletion region forming a nonlinear capacitance. The motion of the depletion layer edge depends on the motion of the electrons in the bulk quasi-neutral region. The goal is to have high mobility high velocity electrons in the region. This is the typical condition at lower frequencies and RF voltages where the amount of displacement current that the bulk region must support is reasonable. However, as the RF frequency increases for the same RF drive level, the peak fields in the bulk increase and electron begin to transfer to the upper valley during a portion of the RF cycle and do not have enough time to transfer back during the remaining portion of the cycle. This leads to a decrease in the average velocity of the bulk electrons, a saturation of the velocity through the bulk region and a decrease in the multiplier efficiency. Details of this effect will be described in more detail in section III.

An inductive delay occurs in a material when the electron motion can not follow a rapidly changing electric field. The delay effect can be illustrated with a balance equation relating the time rate change of an electron's velocity as a result of an electric field and a simple momentum relaxation term

$$dv/dt = qE/m^* - v/\tau_m, \tag{1}$$

where v is the velocity,q is the electronic charge,E is the applied field,m^* is the effective mass and τ_m is the momentum relaxation time. Under steady state conditions, the time derivative is zero, and the equation becomes

$$\mu = v/E = q\tau_m/m^* \quad (2)$$

where μ is the carrier mobility. For GaAs the effective mass is $0.068m_0$ and μ is 8500 $cm^2/Vsec$ for lightly doped material giving τ_m around 0.32 picoseconds. The current vs. time through a piece of bulk GaAs in response to a 1000 volt per cm peak to peak sin wave at 500 GHz is shown in Fig. 2.The response of the current to the sinusoidal drive is inductive. GaAs is a useful material for devices because it's high mobility gives a low resistance. However, at frequencies above 500 GHz, the inductive nature of the electron motion or current becomes important. This inductive effect will be discussed further in section IV.

Monte Carlo Simulation of Varactors

The Monte Carlo device simulation described in the last section has been used to study the operation of varactors and mixers. A description of these results will be given in this section. The structures are chosen to illustrate the saturation effects under consideration.

The first device is a GaAs Schottky barrier varactor diode with an epitaxial layer doping of $3 \times 10^{16}/cm^3$, an epitaxial layer length of 1.25 $\mu meter$ and a $0.25\mu meter$ long contact doped at $10^{17}/cm^3$. These parameters correspond to a relatively low frequency, high breakdown voltage device. All the plots are normalized to an area of one cm^2. The voltages all refer to voltages across the semiconductor excluding the built- in voltage of the Schottky barrier, so zero volts corresponds to flat band. The Monte Carlo device is pumped with a single frequency RF voltage with a DC bias and the resulting device conditions are investigated.

The "capacitance" of the varactor as a function of RF phase for a DC bias of -10.5 volts, RF voltages of 2,4,6,8 and 10 volts and frequencies of 100 and 200 GHz is shown in Fig. 4a and Fig. 4b and the fraction of Γ electrons is shown in Fig. 4c and Fig. 4d. The "capacitance" is defined using the depletion layer approximation. The number of electrons in the device changes as a function of time. The number of missing electrons corresponds to an effective depletion layer thickness, and to a "capacitance". An additional "capacitance" associated with the time varying field and out of phase current in the neutral region will add an additional capacitance to the terminal characteristics.

The device capacitance vs. time at 100 GHz is similar to results that would be obtained using under static conditions. The fields in the undepleted portion are low enough that valley transfer doesn't occur for the first four RF voltage levels. Valley

transfer effects due to high electric fields begin to occur for the 10 volt RF voltage case. Cool contact electrons are pulled into the device in the first half of the RF cycle and heated. These heated electrons are then pushed out between 180 and 360°. The maximum time derivative of the terminal voltage is at 270°, so the valley fraction is smaller there. There is reasonable valley fraction modulation. The 100 GHz frequency under consideration corresponds to a period of 10 picoseconds. There is enough time for the electrons that have transferred in the second half of the cycle to relax to the Γ valley for the following lower voltage bias conditions.

The results are different for 200 GHz modulation. Since the frequency is higher a simple scaling would require twice as much current. However, the light doping in the undepleted region will not support the required current. Valley transfer occurs during a portion of the RF cycle. This reduces the velocity and the depletion layer width modulation. Since the depletion layer is narrower than in the 100 GHz case, the neutral region fields are higher. This causes additional transfer. The upper valley electrons do not have time to return to the higher mobility lower valley is the 5 picosecond time scale. These valley transfer effects increase the ohmic loss in the structure. Fig. 4 shows the loss $\frac{1}{2\pi}\int I(t)V(t)dt$ for the two frequencies. The rapid increase in the ohmic loss is due to the higher resistive loss in the lightly doped material.

One way to overcome some of these problems is to increase the doping. Capacitance results for a varactor doped at $9^{16}/cm^2$ with an epitaxial layer $0.8\mu m$ long is shown in Fig. 5a and b and the corresponding valley fraction results are shown in Fig. 5c and d. This structure works much better, but there is still a reduced valley fraction for the 200 GHz modulation. Again, electrons in the neutral region that transfer to upper valleys do not have enough time to transfer back, so there is a buildup of low mobility electrons over several RF periods. Careful characterization will be needed to optimize structures for different RF drive levels and frequencies.

Monte Carlo Simulation of Mixers

The Monte Carlo simulation has also been to start an investigation of limitations in mixers. Mixers are needed at higher frequencies than multipliers, they are usually operated in forward bias, so the capacitance per unit area is higher, and the structure must support both the displacement and injected current. A simulation of a mixer diode with a doping of $1 \times 10^{17}/cm^3$ and a $0.1\mu m$ long epitaxial layer is shown in Fig. 6. It is driven with a 0.5 volt RF voltage at a -0.5 volt bias point. The 180° phase point corresponds to "flatband". The terminal current vs. phase is shown in Fig. 6a. There is a strong inductive effect in this plot, with the inductive delay of the electrons in the neutral region resonating with the depletion layer capacitance. The resulting injected current, or electron current across the Schottky barrier is shown in Fig. 6b. The injected current is delayed about 45° from the "flatband" bias point at 180°. The

peak current is limited by the supply of electrons through the neutral region. The electron energy vs. phase is shown in Fig. 6c. The electrons are being heated by the high electric fields in the device, even though the total voltage across the device is modest. The peak energy of almost 100 milli electron volts occurs near the 270 ° phase point where the current is largest. The time derivative of the terminal voltage is largest at the 90° and 270° phase point. At 90° cool electrons are being pulled into the device from the contact. At 270o hotter electrons are being pushed out. Even with low bias voltages, the electrons are being heated enough to allow valley transfer, as shown in the Fig. 6d. The electrons are heated over several RF cycles, with slow energy loss.

Some of the results in Fig. 6 occur because the structure limits the current. Results for a similar structure with a doping of $2 \times 10^{17}/cm^3$ are shown in Fig. 7. The injected current peak is much higher, but is still shifted by the inductive delay. Since the doping is higher, the resistance in the neutral region is smaller, and there is less damping of the terminal current waveform. The electron energies are smaller and the valley fraction is larger.

Conclusions

This paper has briefly discussion the Monte Carlo simulation of Schottky barrier varactors and mixers. This description shows several important limitations in the operation of these devices beyond the saturation effects discussed in earlier literature. GaAs varactors operating about 100 GHz are limited by valley transfer effects. There is an accumulation of hot electrons in the neutral region of the device in the high voltage portion of the RF cycle. These electrons do not have enough time to thermalize in the remaining portion of the cycle. This will increase the resistance and reduce the performance. The problem can be reduced by not overcome with increased doping. GaAs mixers also have current saturation effects. The bulk region of the device must support both the injected and the displacement current. In addition, an inductive current delay causes an under damped resonant current flow at the device terminals. This current flow heats the electrons and causes valley transfer, increasing the device resistance. These effects will modify the device performance in circuits. The next step is to included these physical effects into a device model that can be used in a nonlinear circuit simulation.

List of Figures

1. Fig. 1 a. Time Response of Electron Γ valley Fraction, b. Electric Field vs. Time for 50 picosecond simulation, c. Time Response of Electron Γ valley Fraction, d. Electric Field vs. Time for 20 picosecond simulation.

2. Fig. 2a. Electric field vs. time b., Current vs. Time for 500 GHz simulation.

3. Fig. 3 a. 100 GHz capacitance vs. time for RF voltages of 2,4,6,8 and 10 volts, b. 200 GHz capacitance vs. time for RF voltages of 2,4,6,8 and 10 volts, c. 100 GHz valley fraction vs. time and d. 200 GHz valley fraction vs. time for $3 \times 10^{16}/cm^3$ structure.

4. Fig. 4 Ohmic loss vs. RF voltage at 100 and 200 GHz.

5. Fig. 5 a. 100 GHz capacitance vs. time for RF voltages of 2,4,6,8 and 10 volts, b. 200 GHz capacitance vs. time for RF voltages of 2,4,6,8 and 10 volts, c. 100 GHz valley fraction vs. time and d. 200 GHz valley fraction vs. time for $9 \times 10^{16}/cm^3$ structure.

6. Fig 6 a. 1 THz terminal current, b. Injected current c. Electron energy and d. Valley fraction for a $1 \times 10^{17}/cm^3$ doped Schottky barrier mixer with RF voltage of 0.5 volts and bias of -0.5 volts.

7. Fig 7 a. 1 THz terminal current, b. Injected current c. Electron energy and d. Valley fraction for a $1 \times 10^{17}/cm^3$ doped Schottky barrier mixer with RF voltage of 0.5 volts and bias of -0.5 volts.

References

1. Siegel, P., Kerr, A, and Hwang,W. ,"Topics on the Optimization of Millimeter Wave Mixers," NASA Technical Paper 2287, March 1984.

2. Microwave Mixers, S.A. Maas, Artech House, 1986.

3. Commerical software includes Harmonica, a product of Compact Software and Libra, a product of HP/EESOF.

4. "Current Saturation in Submillimeter Wave Varactors," by E.Kollberg, T. Tolmunen, M. Frerking and J.East presented at the Second International Conference on Space Terahertz Technology, Pasadena, California, March 1991 with an extended version in *IEEE Trans. on Microwave Theory and Techniques*, Vol. MTT-40, pp. 831-838, 1992..

5. "On the Modeling and Optimization of Schottky Varactor Frequency Multipliers at Submillimeter Wavelengths," by J. Louhi and A. Raisanen, presented at the Fifth International Conference on Space Terahertz Technology, Ann Arbor, Michigan, May, 1994.

6. Crowe,T., Peatman,W., Zimmermann,R. and Zimmermann, R.,"Consideration of Velocity Saturation in th Design of GaAs Varactor Diodes," *IEEE Microwave and Guided Wave Letters*, vol. 3, No. 6, pp 161-163, June, 1993.

7. "Performance Limitations of Varactor Multiplies," by J. East, E.Kollberg and M. Frerking presented at the Fourth International Conference on Space Terahertz Technology, Los Angles, California, March 1993.

8. Non-Ohmic Transport in Semiconductors by W. Fawcett in Electrons in Crystalline Solids, International Atomic Energy Agency, Vienna 1973.

9. Computer Simulation Using Particles by R.Hockney and J.Eastwood, McGraw Hill, 1981.

10. U. Bhapkar and R. Mattauch, " Time-Dependent Monte Carlo Simulation of Schottky Diodes at Terahertz Frequencies," 1993 International Semiconductor Device Research Symposium, Charlottesville, Virginia, Dec. 1993, pp 381-384.

11. Bosch,R. and Thim,H., "Computer Simulation of The Transferred Electron Effect Using the Displaced Maxwellian Approach," *IEEE Trans. on Electron Devices* Vol. ED-21, No. 1 pp 16, Jan. 1974.

12. Kroemer,H., "Hot-Electron Relaxation Effects in Devices," *Solid State Electronics*, Vol. 21,pp 61-67, 1978.

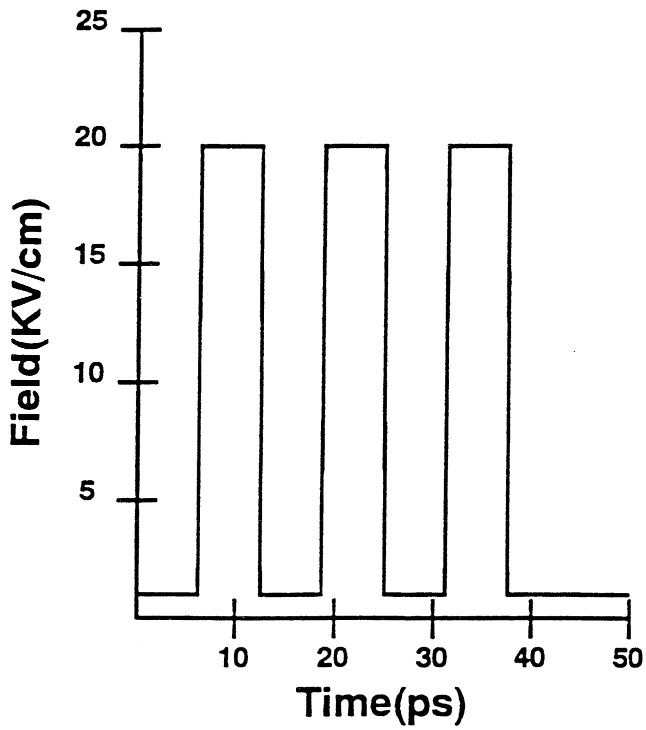
(a) Field vs. long time
Field(KV/cm)
25
20
15
10
5
10
20
30
40
50
Time(ps)

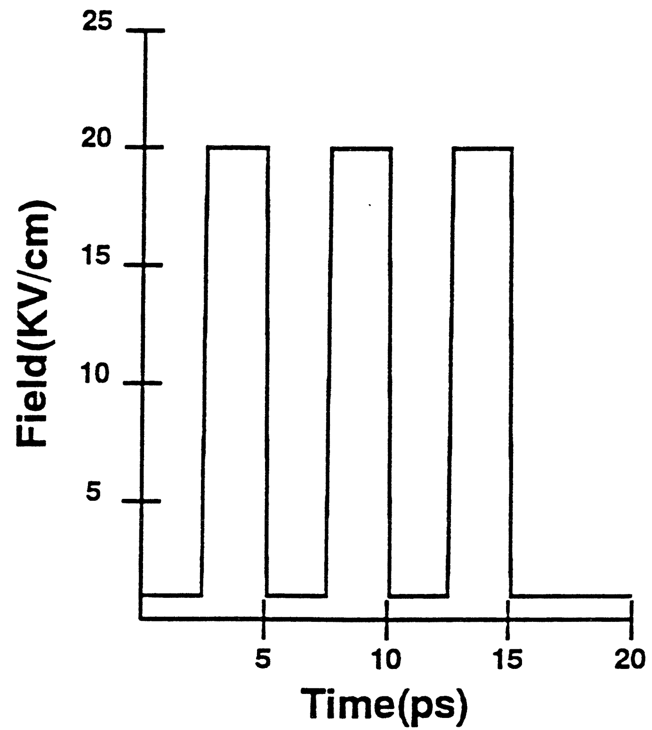
(c) Field vs. short time
Field(KV/cm)
25
20
15
10
5
5
10
15
20
Time(ps)

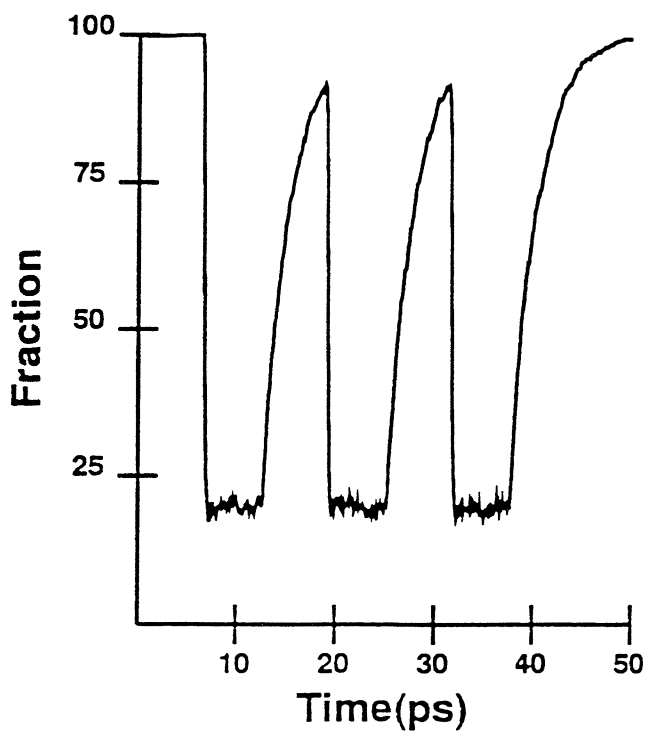
(b) Valley fraction vs. long time
Fraction
100
75
50
25
10
20
30
40
50
Time(ps)

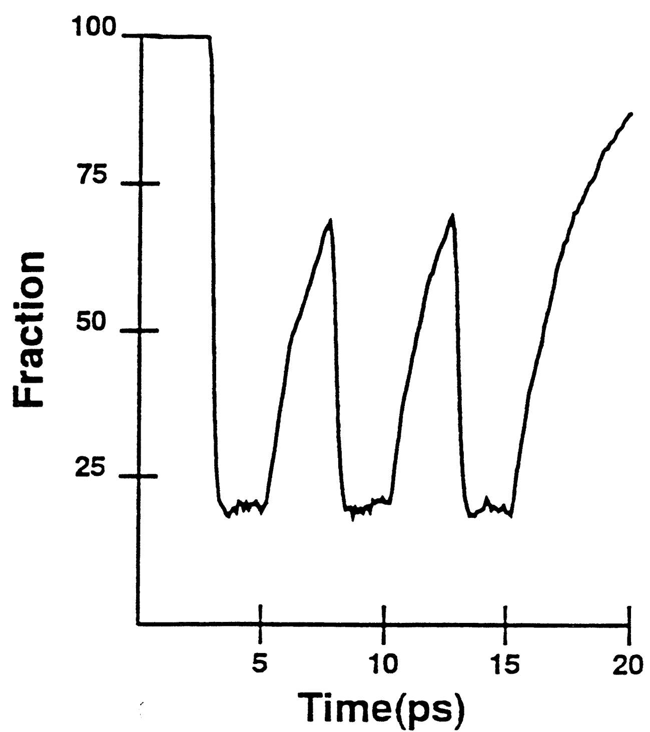
(d) Valley fraction vs. short time
Fraction
100
75
50
25
5
10
15
20
Time(ps)

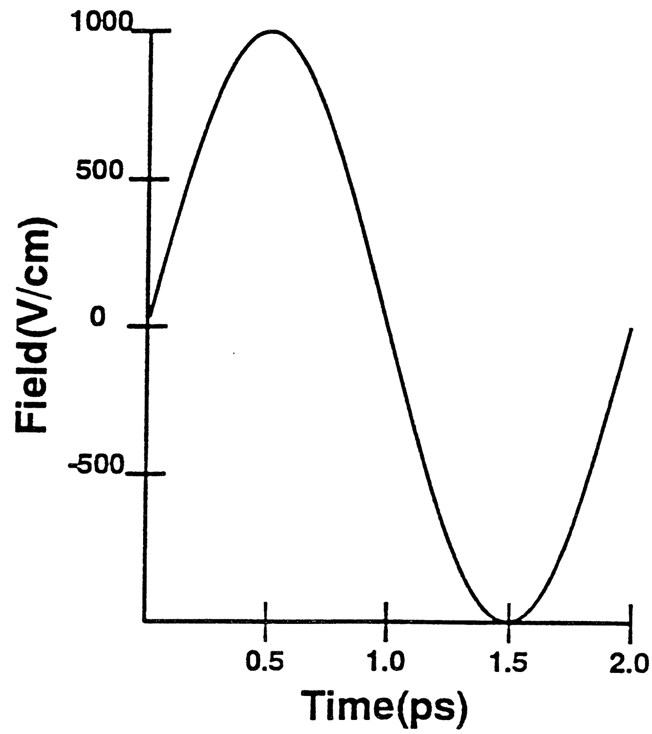
(a) Field vs. time
1000
500
0
-500
Field(V/cm)
0.5
1.0
1.5
2.0
Time(ps)

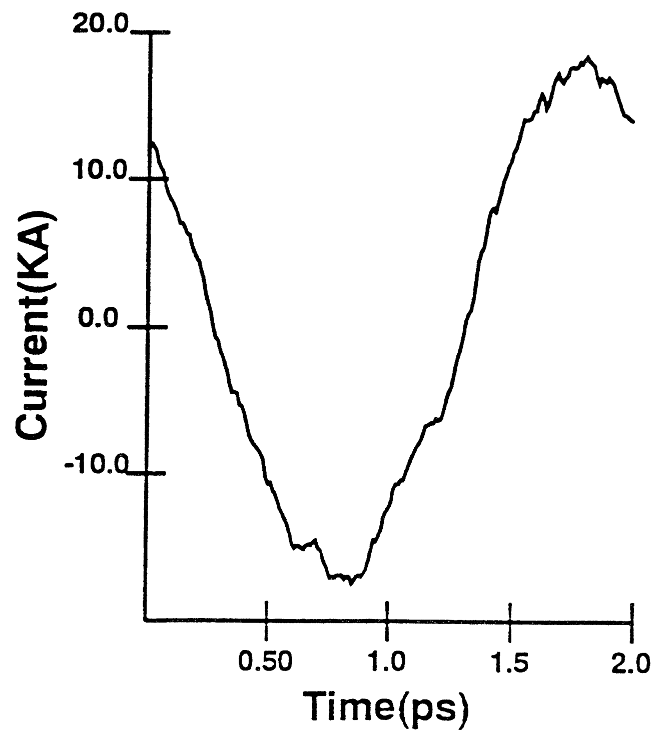
(b) Current vs. time
20.0
10.0
0.0
-10.0
Current(KA)
0.50
1.0
1.5
2.0
Time(ps)

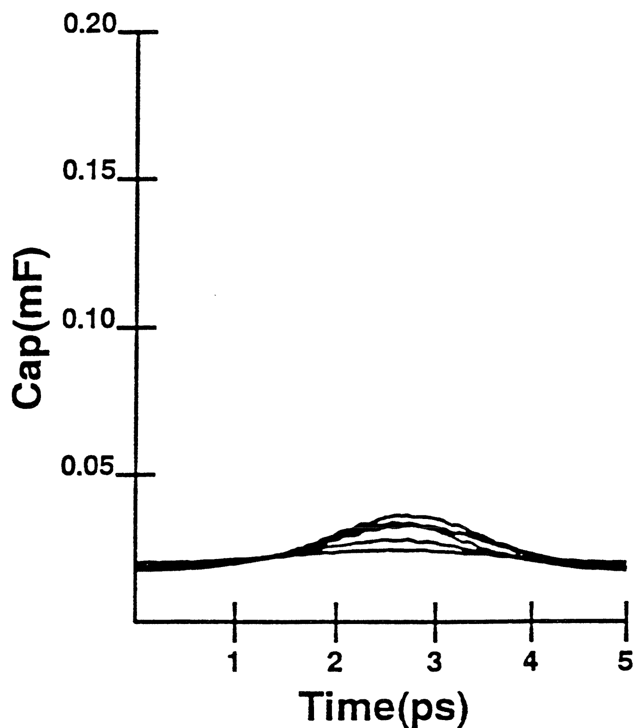
(b) 200 GHz capacitance
0.20
0.15
0.10
0.05
Cap(mF)
1
2
3
4
5
Time(ps)

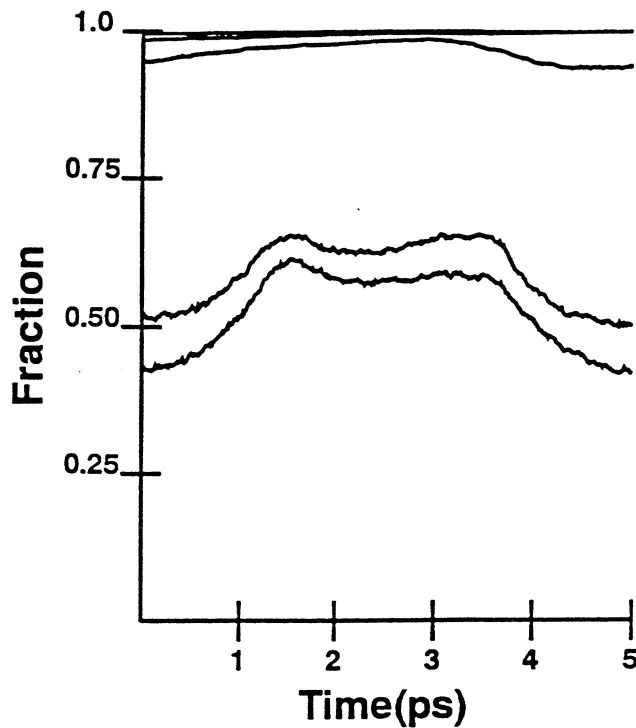
(d) 200 GHz fraction
1.0
0.75
0.50
0.25
Fraction
1
2
3
4
5
Time(ps)

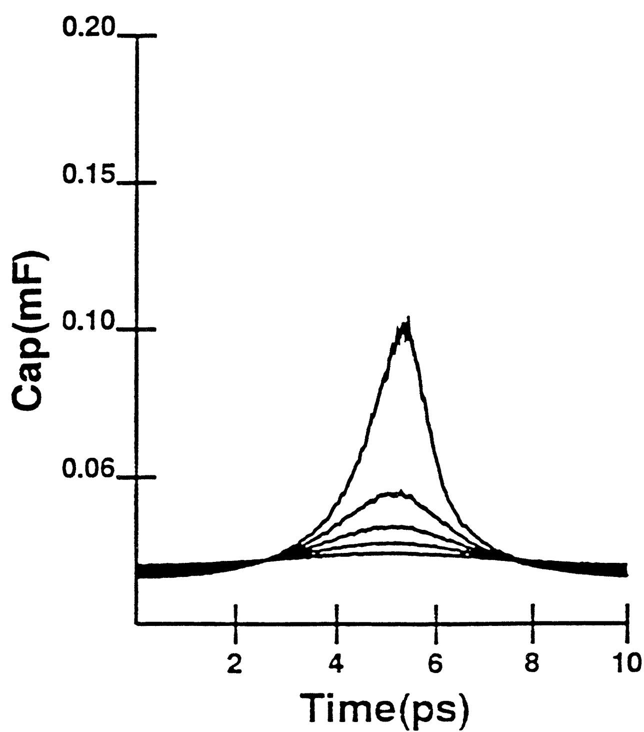
(a) 100 GHz capacitance
0.20
0.15
0.10
0.06
Cap(mF)
2
4
6
8
10
Time(ps)

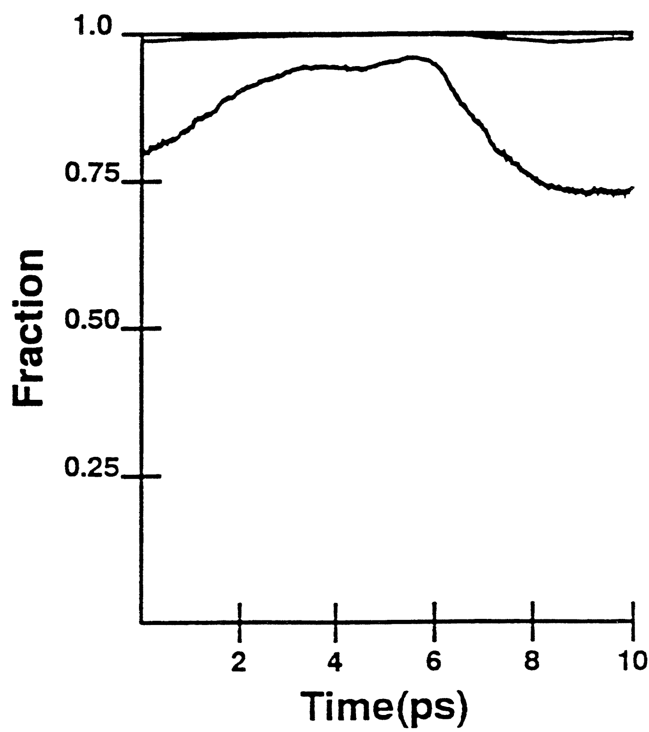
(c) 100 GHz fraction
1.0
0.75
0.50
0.25
Fraction
2
4
6
8
10
Time(ps)

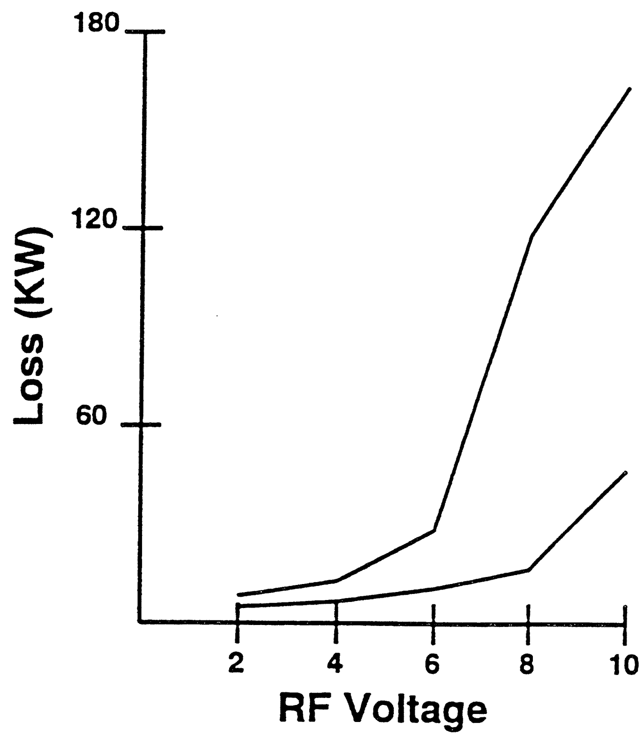
ohmic loss vs. drive level
180
120
60
Loss (KW)
2
4
6
8
10
RF Voltage

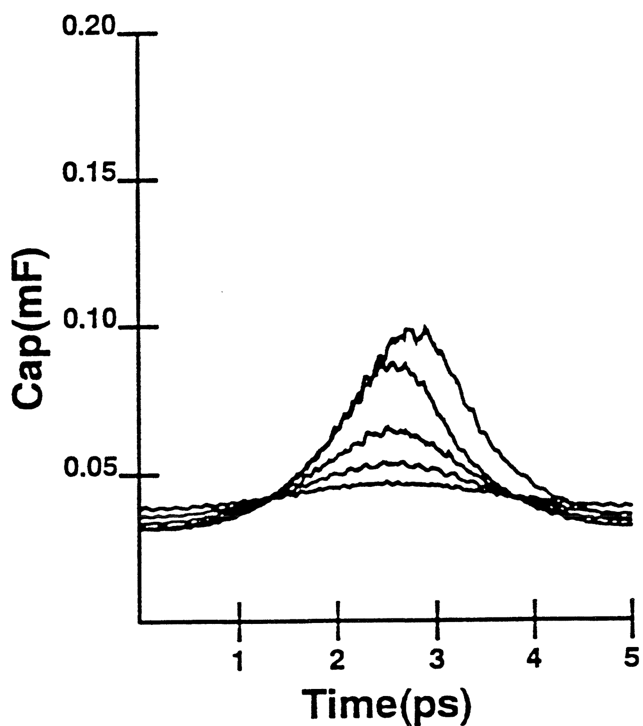
(b) 200 GHz capacitance
0.20
0.15
0.10
0.05
Cap(mF)
1
2
3
4
5
Time(ps)

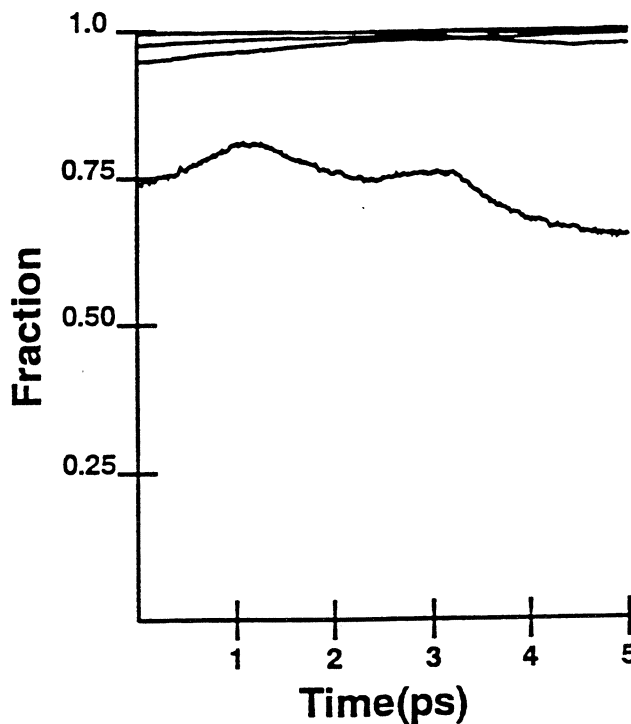
(d) 200 GHz fraction
1.0
0.75
0.50
0.25
Fraction
1
2
3
4
5
Time(ps)

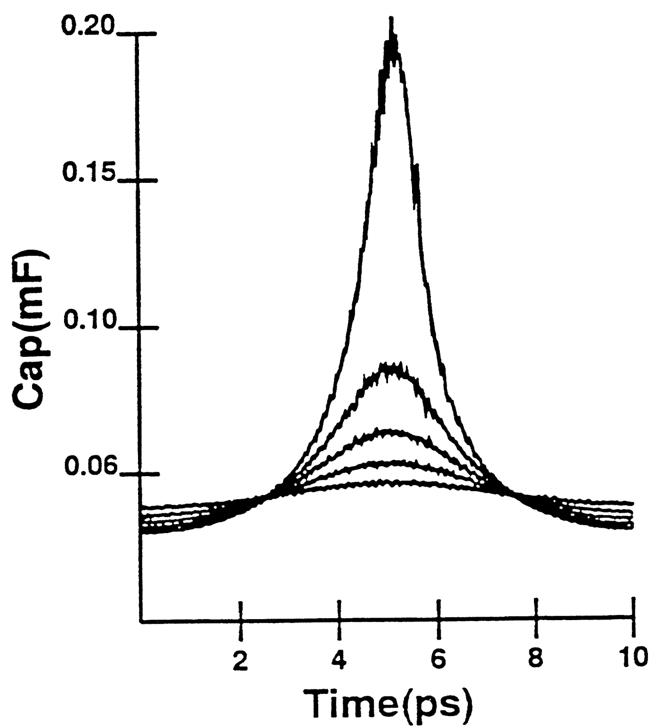
(a) 100 GHz capacitance
0.20
0.15
0.10
0.06
Cap(mF)
2
4
6
8
10
Time(ps)

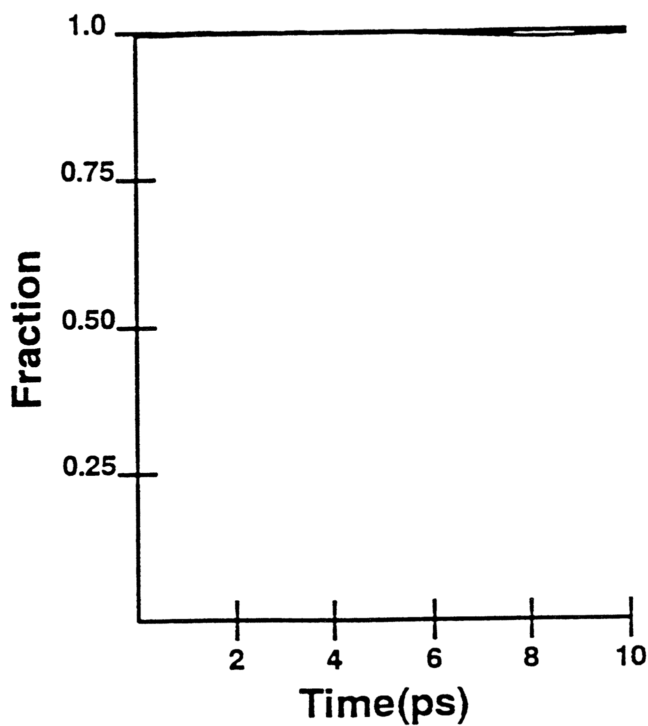
(c) 100 GHz fraction
1.0
0.75
0.50
0.25
Fraction
2
4
6
8
10
Time(ps)

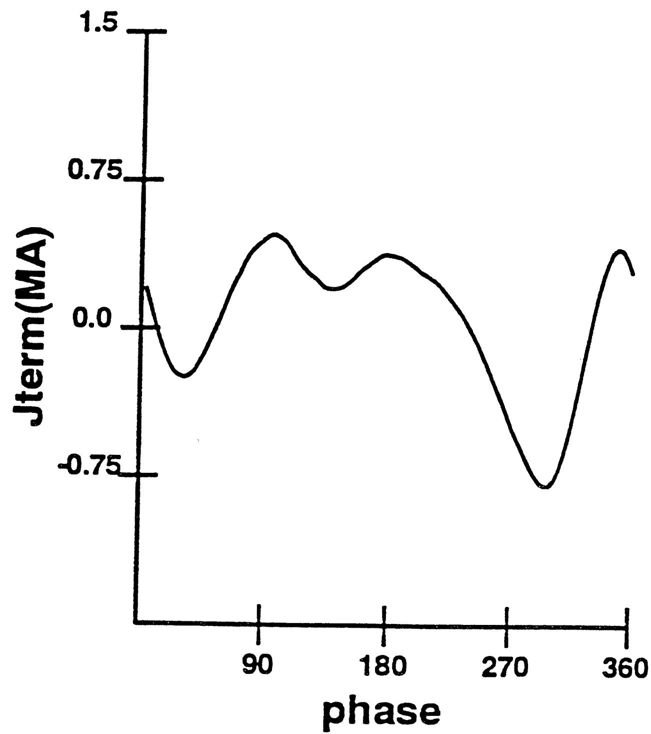
(a) 1 THz terminal current vs. phase
1.5
0.75
0.0
-0.75
Jterm(MA)
90
180
270
360
phase

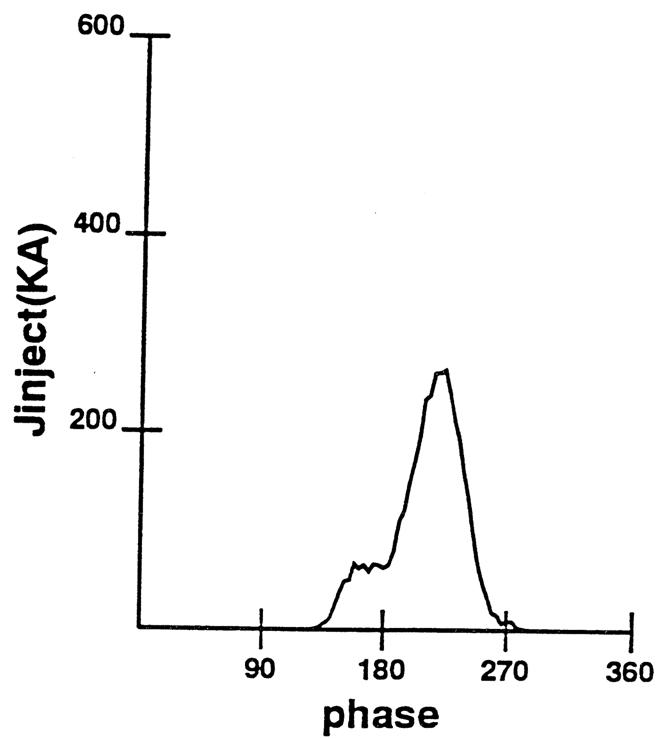
(b) 1 THz injected current vs. phase
600
400
200
Jinject(KA)
90
180
270
360
phase

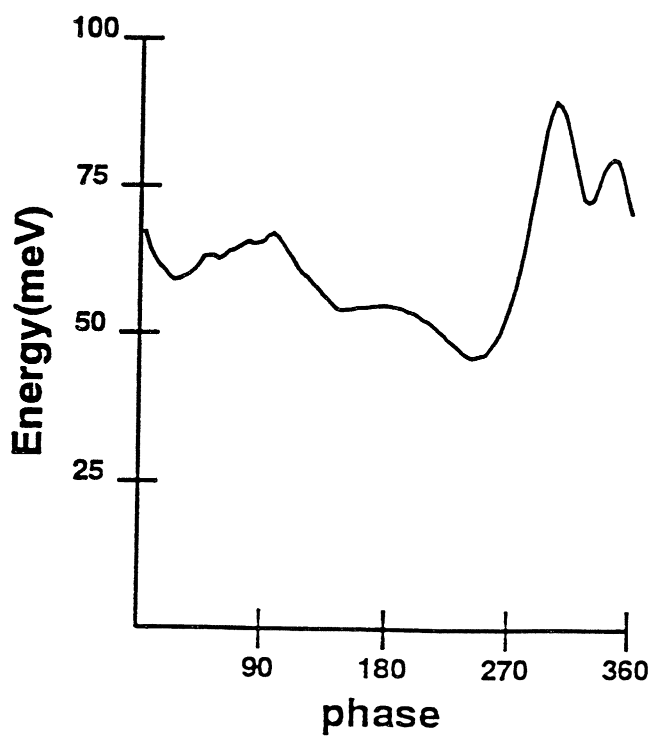
(c) 1 THz energy vs. phase
100
75
50
25
Energy(meV)
90
180
270
360
phase

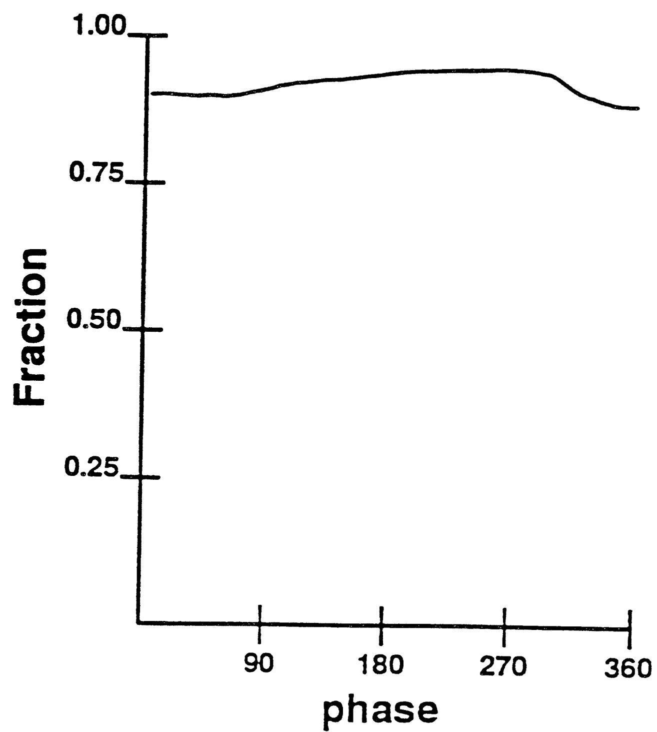
(d) 1 THz fraction vs. phase
1.00
0.75
0.50
0.25
Fraction
90
180
270
360
phase

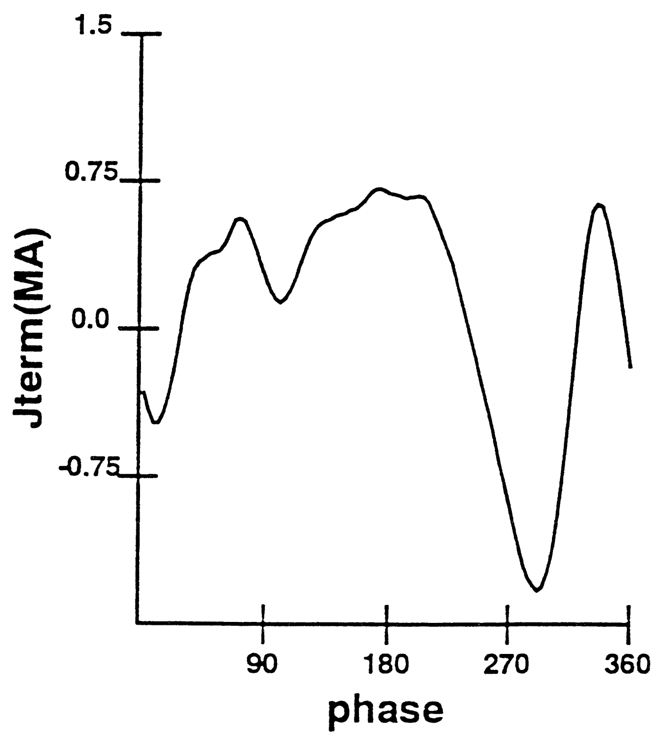
(a) 1 THz terminal current vs. phase
1.5
0.75
0.0
-0.75
Jterm(MA)
90
180
270
360
phase

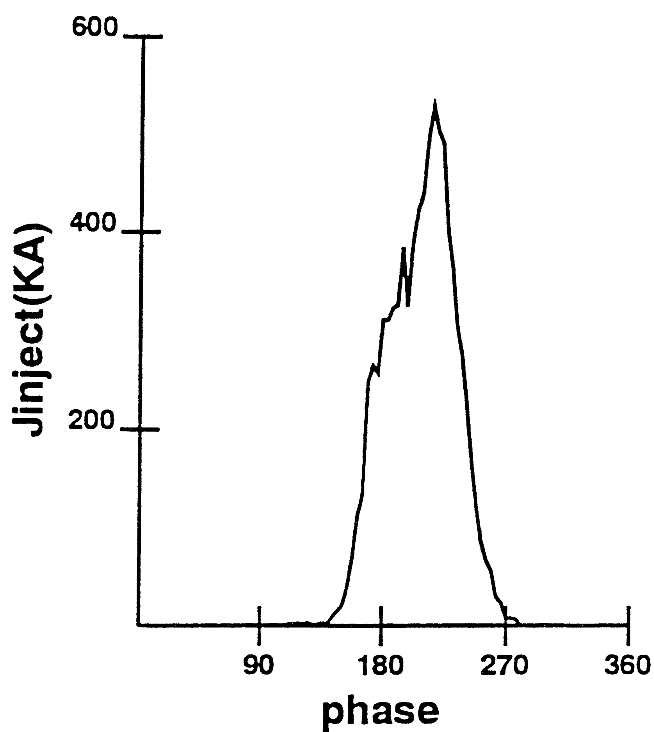
(b) 1 THz injected current vs. phase
600
400
200
Jinject(KA)
90
180
270
360
phase

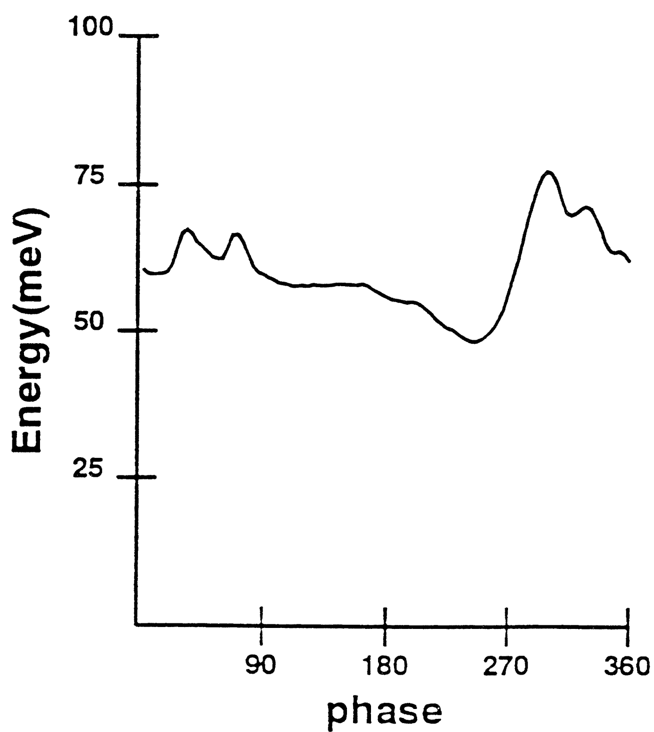
(c) 1 THz energy vs. phase
100
75
50
25
Energy(meV)
90
180
270
360
phase

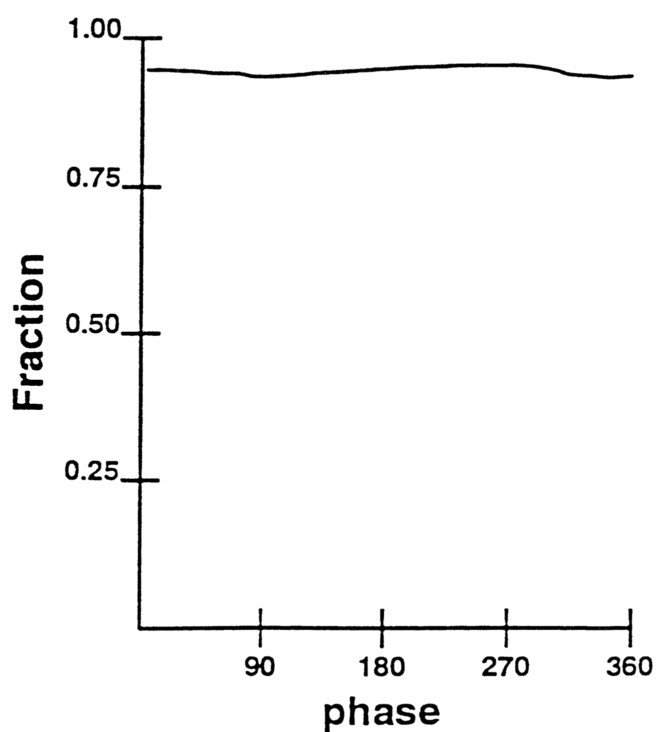
(d) 1 THz fraction vs. phase
1.00
0.75
0.50
0.25
Fraction
90
180
270
360
phase